PHYSICAL REVIEW C **69**, 011602(R) (2004)

Pre-emission of correlated neutrons in the fusion of ^{11}Li halo nuclei with Si targets

M. Petrascu, A. Constantinescu,* I. Cruceru, M. Giurgiu,† A. Isbasescu, M. Isbasescu, H. Petrascu, and C. Bordeanu‡
Horia Hulubei National Institute for Physics and Nuclear Engineering, P.O.B. MG-6, Bucharest, Romania

I. Tanihata, T. Kobayashi,§ K. Morimoto, K. Katori, M. Chiba, Y. Nishi, S. Nishimura, A. Ozawa, T. Suda, and K. Yoshida
RIKEN, Hirosawa, 2-1, Wako, Saitama 351-0198, Japan
(Received 29 August 2003; published 30 January 2004)

The recent experiment with a new array detector aiming the investigation of halo neutron pair pre-emission in Si(^{11}Li, fusion) is described. A new approach for testing the true *n-n* coincidences against cross-talk has been worked out. An experimental evidence for residual correlation of the pre-emitted halo neutrons is presented. The results obtained in building the *nn* correlation functions by using the available denominators are discussed. A recent iterative method for calculation of the intrinsic correlation function was also applied. An experiment for precise measurement of the intrinsic *nn* correlation function is proposed.

DOI: 10.1103/PhysRevC.69.011602 PACS number(s): 25.60.Pj, 27.20.+n

The neutron halo nuclei were discovered by Tanihata and co-workers [1]. These nuclei are characterized by very large matter radii, small separation energies, and small internal momenta of valence neutrons. Recently it was predicted [2] that, due to the very large dimension of ^{11}Li, one may expect that in a fusion process on a light target the valence neutrons may not be absorbed together with the ^{9}Li core, but may be emitted in the early stage of the reaction. Indeed, the experimental investigations of neutron pre-emission in the fusion of ^{11}Li halo nuclei with Si targets [3,4] have shown that a fair amount of fusions $(40\pm12)\%$ are preceded by one or two halo neutron pre-emission. It was also found that in the position distribution of the pre-emitted neutrons, a very narrow neutron peak, leading to transverse momentum distribution much narrower than that predicted by cluster orbit shell model approximation (COSMA) model [5], is present.

Some indication based on preliminary *n-n* coincidence measurements, concerning the presence of neutron pairs within the narrow neutron peak, has been mentioned in Refs. [3,4]. In the light of this indication, the narrow neutron distribution could be caused by the final state interaction [6,20] between two pre-emitted neutrons. Therefore, on the basis of these first results, it was decided to perform a new experiment aiming to investigate the neutron pair pre-emission in conditions of much higher statistics, by means of a neutron array detector. This experiment has been performed at the RIKEN-RIPS facility. The experimental setup is shown in Fig. 1. In this setup, three main parts are present: The first part contains the detectors used for the beam control: a thin scintillator at the F2 focus of the RIPS, two parallel plate avalanche counters (P1,P2) and a V1(Veto1) scintillator, provided with a 2×2 cm^2 hole. The second part consists of a MUSIC chamber [7], containing inside a 500 μm thick strip silicon detector target (SiS) and a V2(Veto2) Si detector, 200 μm thick. MUSIC was used for the identification of the inclusive evaporation residues spectra produced in the detector target, and for suppression of the energy degraded beam particles. The third part is the neutron array detector [8,14]. It consists of 81 detectors, made of $4\times4\times12$ cm^3 BC-400 crystals, mounted on XP2972 phototubes. This detector, placed in the forward direction at 138 cm from the target, was used for the neutron energy determination by time of fight and for neutron position determination. The distance between adjacent detectors was 0.8 cm. The array components were aligned to a threshold of 0.3 MeVee (MeV electron equivalent), by using the cosmic ray peak at 12 MeV (8 MeVee). The numbering of the detectors was performed in the following way: The central detector was labeled 1. The eight detectors surrounding detector 1, were labeled counterclock wise 2–9. The second circle of 16 detectors were labeled 10–25 and so on. In the present paper the coincidences between adjacent detectors are denoted as "first order coincidences." Coincidences between two detectors separated by one detector are denoted as "second order coincidences" and so on. With the trigger specified in Fig. 1 caption, one could investigate inclusively the ^{9,11}Li+Si fu-

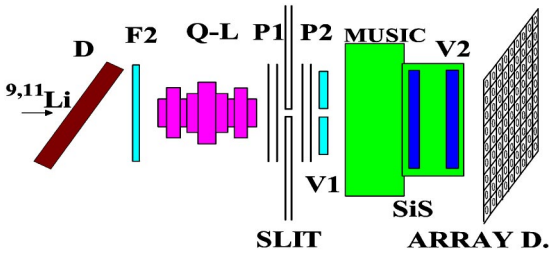

FIG. 1. (Color online) The general setup of the experiment. Detectors F2, P2, V1(Veto1), SiS, V2(Veto2) were used in the trigger: F2×P2×*Veto*1×SiS×*Veto*2. MUSIC was used for suppression of the energy degraded beam (see text). The neutron array detector consisting of 81 modules was placed in forward direction at 138 cm from the target.

*Permanent address: University of Bucharest, Bucharest, Romania.
†Permanent address: Technical University, Bucharest, Romania.
‡Present address: CENPA, Washington University, Washington USA.
§Permanent address: Tohoku University, Tohoku, Japan.

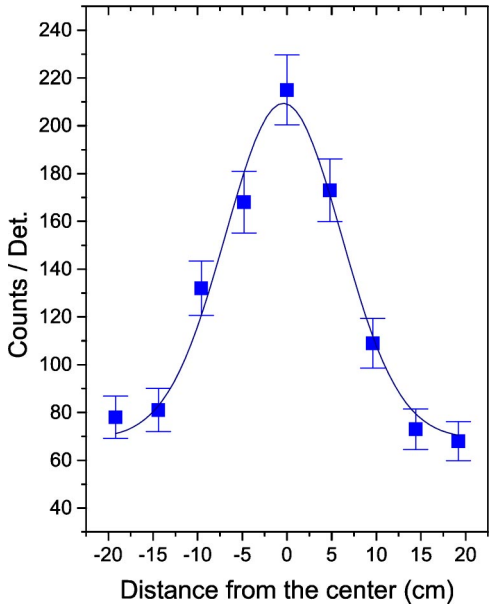

FIG. 2. (Color online) The position spectrum measured along the horizontal line connecting detectors 58–74 is shown. The neutron energy was selected between 6 and 16 MeV. The FWHM of this spectrum is ~13 cm and corresponds to a solid angle ~9 msr.

sion. The large 5×5 cm^2 silicon Veto2 detector, placed behind the Si-strip target detector, eliminated the elastic, inelastic, and breakup processes at forward angles. The measurements were performed with 13*A* MeV ^{11}Li and ^{9}Li beams. The energy range corresponding to the neutron pre-emission process was established between ~8 and ~15.5 MeV [9].

In Fig. 2, the position spectrum measured along the horizontal line connecting detectors 58–74 is shown. The neutron energy was selected between 6 and 16 MeV. The full width at half maximum (FWHM) of this spectrum is ~13 cm and corresponds to a solid angle of ~9 msr. Within this narrow peak, a large number of *n*-*n* coincidences were observed for ^{11}Li [10] by comparing the data obtained with ^{11}Li and with ^{9}Li beams.

In this paper, the criterion [11,12] for selecting the true coincidences against cross-talk (c.t.) was adopted. Cross-talk is a spurious effect in which the same neutron is registered by two or more detectors. A coincidence between two detectors is rejected whenever the following condition is fulfilled:

$$E_1 > E_{min} = \frac{1}{2} m \frac{d_{min}^2}{(t_2 - t_1)^2}. \quad (1)$$

Here E_1,t_1 are the energy and the arrival time of the first neutron. E_{min} is the minimum energy required by the neutron scattered from the first detector to travel the minimum distance d_{min} to the second detector (arrival time t_2), in the time interval t_2-t_1. For the first rejection we took d_{min} equal to the distance between the detector centers. For example, by applying this criterion to the first order coincidences, a total of 118 true coincidences were found. For further rejection we consider that it is more appropriate to use the d_{min} parameter instead of time of flight, because the distance between the adjacent detector centers is close to the detector dimension. By taking d_{min}=1.8 cm, the number of first order true coincidences is reduced from 118 to 46. We took this distance from a simple geometrical consideration showing that less than 1.5% of the c.t. could pass as true coincidences [18]. The author of MENATE, Desesquelles, has adapted the program [13] for c.t. rejection by using d_{min}. Applying this program, to first order coincidences, it appears that only one c.t. in 3000 can pass as a true coincidence [18]. Thus the upper qualitative estimation is confirmed. As a result of rejection by d_{min}, a sample of 204 true coincidences, including also the higher order ones, was obtained.

The significance of the obtained data was additionally tested through a complete simulation of the array detector performances by using MENATE. We have investigated in this way the c.t. distribution as a function of $t=t_2$-t_1 for different coincidence (first to fourth) orders. The simulation was performed by firing the central detector 1 by neutrons of given energy and by extracting the cross-talk events corresponding to 2–9 detectors (first order), to 10–25 detectors (second order), and so on. For each event, the space and time coordinates and also the light output were available. In these simulations was found the notable fact that, in the case of a cross-talk, ~87% of the events are concentrated in the first half of detector 1, and only ~13% of the events are distributed within the second half of this detector. On the other hand, the events in detector 2 (here by detector 2 is understood whatever c.t. partner of detector 1) are distributed ~87% within the second half and only ~13% within the first half. This effect is interpreted as being due to the predominance of the neutron scattering cross section in the forward direction. In the case of a single-neutron detection, about 63% of the events occur within the first half and about 37% within the second half. The observed behavior of c.t. causes a notable suppression of short neutron trajectories between detectors 1 and 2. For example, in 1000 c.t. events there are no trajectories shorter than 1.8 cm. The number of 1.8 cm trajectories is less than 5 in 1000 c.t. events. Due to this concentration of events caused by c.t., appears a remarkable improvement of σ_{t1} time resolution of detector 1. This resolution has to be understood as being related to the finite detector thickness. We obtained that σ_{t1}=0.53 ns, 0.59 ns, 0.63 ns for, respectively, 15 MeV, 11 MeV, and 8 MeV neutron energy. In the absence of c.t., that is, for single-neutron detection, the corresponding resolutions are 0.7 ns, 0.8 ns, and 0.9 ns, respectively. Thus the resolution in the presence of first order c.t. is improved ~1.4 times.

In Fig. 3, the experimental *n*-*n* coincidence (true and c.t.) are denoted by open up-triangles with uncapped error bars. The distribution of simulated first order c.t. as a function of t_2-t_1 is indicated by solid squares with capped error bars. The simulations were performed by taking three different neutron energies: 8, 11, and 15 MeV, representing, respectively, the lower limit, peak, and upper limit of the neutron pre-emission spectrum. A total of 1000 c.t. were calculated in each case. The calculated c.t. spectra were normalized to the mean of experimental points in the peak range of the calculated spectra. One may see that in all three figures (a)–(c) there is a window, denoted by TC (true coincidences), in

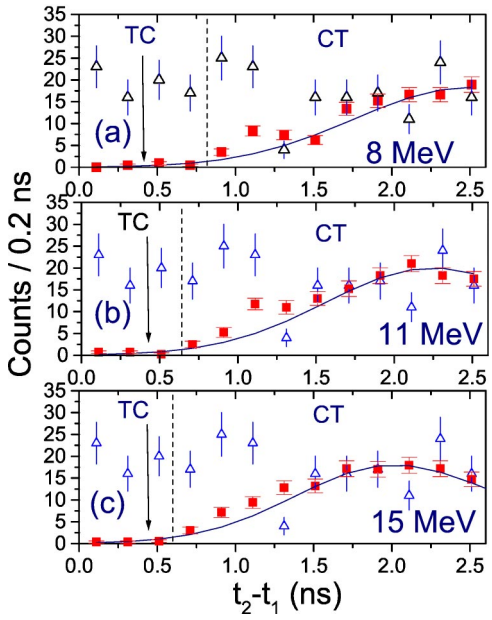

FIG. 3. (Color online) Monte Carlo simulation of the first order c.t. The open up-triangles with uncapped error bars represent the experimentally measured coincidences. The solid squares with capped error bars represent the simulated c.t. For details see text.

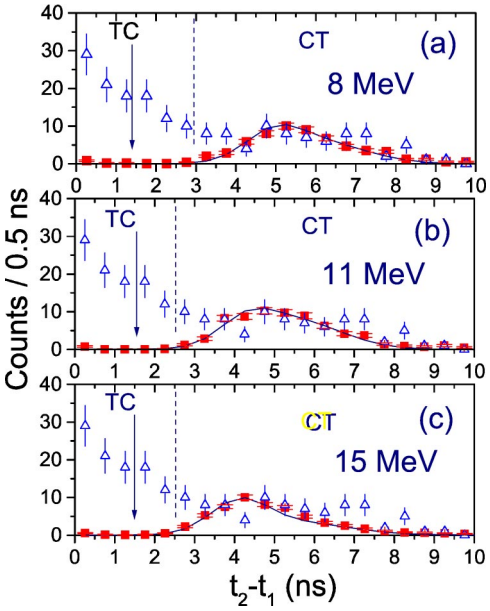

FIG. 4. (Color online) Monte Carlo simulation of the second order c.t. The open up-triangles with uncapped error bars represent the experimentally measured coincidences. The solid squares with capped error bars represent the simulated c.t. For details see text.

which the yield of c.t. is very low (near 0.1 counts). The width of the TC window is the same (0.6 ns) for 11 and 15 MeV and is larger (0.8 ns) for 8 MeV neutrons. TC is separated by a vertical dotted line from the c.t. (cross-talk) window in which c.t. yield is much larger. The first c.t. point in the c.t. window is higher by a factor ~10 than the c.t. points in TC window. This means that a change in the c.t. mechanism is taking place by passing from the c.t. to the TC window. A two-parameter (time-trajectory length) analysis shows that in the majority of events the trajectory length in TC window is larger than ~6 cm. Since a neutron cannot cover this distance in such a short time, it follows that c.t. is realized in the TC window predominantly by γ rays. This explains also why c.t. yield is so low in the TC window. The vertical arrows in Fig. 3, indicate that the remaining 46 true coincidences after d_{min} rejection are well inside the TC window.

Trying to analyze the simulated c.t. distribution we found that it is not possible to use a single Gaussian, due to the presence of a queue at large t_2-t_1 values. Therefore an analysis by means of two Gaussians was used. The resulted total fit corresponds to $\sigma_t \sim 0.6$ ns on the left branch shown in Fig. 3 (beginning from the peak towards lower t_2-t_1 values). The right hand branch (not shown in Fig. 3) corresponds to $\sigma_t \sim 1$ ns. In order to make a comparison with experimental data one has to add to the simulation data the scintillator and electronic resolution which is estimated to be ~0.4 ns (for two detectors). This will increase σ_t by ~0.1 ns and therefore the correction in the TC window should be negligible. A more detailed discussion about a relative independence on σ_t resolution of the TC window and about the applicability of corrections in this window will be done elsewhere [14].

In Fig. 4, the c.t. simulation for second order coincidences is shown. One may see that the number of true coincidences (71) remaining after d_{min} rejection is also well inside the TC window. In this figure the entire c.t. peak is shown. It is remarkable that MENATE program is able to describe fairly well the experimental c.t. distribution. The two Gaussian fit leads in the case of the left branch to a σ_t value close to the corresponding one for first order coincidences. In the case of the right branch, σ_t is by ~20% higher than the corresponding first coincidence value. We have found for second order c.t. that σ_{t1} is improved ~1.7 times.

In the case of third and fourth order coincidences there is correspondingly an increase by 1 ns and by 2 ns of the TC window in comparison with the second order coincidences [14]. In both these cases the true coincidences resisting d_{min} rejection are also well inside the TC window. In conclusion, the performed simulation confirms the validity of the data obtained by d_{min} rejection [14].

The two-neutron correlation function [15] is given by

$$C(q) = k\frac{N_c(q)}{N_{nc}(q)}. \qquad (2)$$

In Eq. (2), $N_c(q)$ represents the yield of coincidence events and $N_{nc}(q)$ represents the yield of uncorrelated events. The normalization constant k is obtained from the condition that $C(q)=1$ at large relative momenta. The relative momentum q is given by $q=1/2|\mathbf{p}_1-\mathbf{p}_2|$, $\mathbf{p}_1$ and $\mathbf{p}_2$ being the momenta of the two coincident neutrons.

A crucial problem for getting the correlation function is the construction of the denominator in formula (2). A thorough analysis of this problem is presented in Refs. [12,16]. Two approaches are commonly used: one is the event mixing technique, the other is the single-neutron product technique.

In the event mixing approach the denominator is generated by randomly mixing the neutrons from the coincidence sample. This method has the advantage that the uncorrelated distribution corresponds to the same class of collisions and kinematic conditions as in the case of the numerator, but has the disadvantage that it may distort the correlation one wants to measure, because the event mixing technique may not succeed to decorrelate completely the events. In the single product technique the denominator is constructed by the product of single-neutron distributions. This method is preferred in Refs. [12,16], considering that the background in this case is truly uncorrelated; but this is not valid for the halo neutrons [17], because of residual correlation. In Ref. [17] it was assumed that residual correlation in the case of halo neutrons should exist due to the large value of $C(q) \sim 10$, and therefore an iterative calculation was applied in order to get a reasonable value for $C(q)$.

Here we will present an experimental evidence for residual correlation of the halo neutrons pre-emitted in the fusion of ^{11}Li+Si. Essentially we have proven the existence of residual correlation by applying the single product technique in the following situations: (a) By coupling randomly single neutrons and by applying the rejection procedure afterwards [12,16]; (b) by replacing the neutrons in the coincidence sample with neutrons with closest energies from the single-neutron sample, corresponding to the same detectors as in the coincidence sample. The condition of closest energies is equivalent to the rejection procedure used in condition (a). This is because the true coincidence sample was obtained by a rejection procedure using the d_{min} parameter. The replacing of the neutrons in the coincidence sample by neutrons with closest energies from the single-neutron sample will keep the initial rejection. This may be seen in Fig. 5(a), in which denominator B (open circles) and the event mixing denominator (crosses) are represented. These two denominators are equal to each other within 1.5%. In this way, both types of denominators A and B will consist of single-neutron products, to which a rejection procedure has been applied. One has also to point out that in both cases, exactly the same number of single products are used. We will show in the following [18] that denominator A presents large fluctuations and is significantly higher than denominator B, when expressed as a function of q in steps of 0.5 MeV/c. In the case when larger steps of q are used (2 MeV/c), denominator A remains significantly higher than B, but displays no more fluctuations. In Fig. 5(c), the solid squares with error bars represent denominator A and the open circles represent denominator B. These denominators are expressed as functions of q in 0.5 MeV/c steps. One may see that denominator A displays fluctuations marked by the vertical lines 1–5, the largest being that marked by vertical line 3. One may also see that denominator $A(q)$ is significantly higher than $B(q)$ at least up to $q \sim 11$, which is the most interesting range for $C(q)$. The ratios $A(q)/B(q)$ corresponding to lines 1–5 have the following values: 1.78, 1.68, 2.0, 1.47, 1.22. One could see that also denominator B presents small fluctuations just as the one marked by line 2, or anomalies as maximum values or turning points for the other lines. This indicates that either the large fluctuations present in A or the small anomalies visible in B are the effect of same interaction more favored by condition (a) than by condition (b). The difference between A and B is due to the fact that in the case of A, more correlated background (residual correlation) than in B is present, because the detectors corresponding to A are in a more central position of the neutron peak, than the detectors corresponding to B [18]. In Fig. 5(b) the denominators A and B are represented as a function of q in steps of 2 MeV/c. One may see, that while the fluctuations seen in Fig. 5(c) completely disappear, the large values of $A(q)$ in comparison with $B(q)$ still remain. The ratios $A(q)/B(q)$ for the first five points, are the following: 1.54, 1.66, 1.54, 1.31, 1.12.

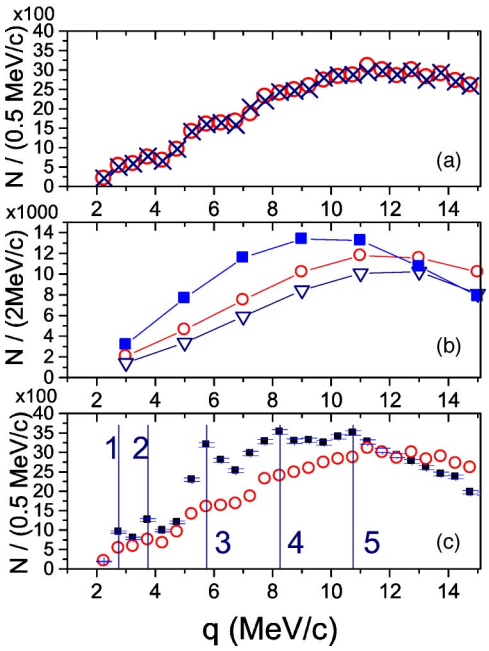

FIG. 5. (Color online) (c): The denominators A (solid squares with error bars) and B (open circles) are represented as a function of q, in 0.5 MeV/c steps. (b): The same denominators are represented as a function of q, in 2 MeV/c steps. By open down-triangles is shown the denominator obtained by iterative calculation [17], starting with B and leading to a correlation function corresponding to $r_0 = 3.3 \pm 0.8$ fm. (a): The denominator B (open circles) and the event mixing denominator (crosses) are represented together, in steps of 0.5 MeV/c.

Concerning the nature of the peak in Fig. 2, in Ref. [10] it was shown that it is due mainly to the pre-emission of neutron pairs. The mechanism determining the appearance of this peak is assumed to be the final state n-n interaction [6,19,20], producing a strong focusing of the pre-emitted neutrons. In the absence of this interaction, the halo neutrons would be distributed according to their internal momentum inside the ^{11}Li nucleus [5], in a 15 times larger forward cone. It follows that the final state n-n interaction changes the initial directions of p momenta. The experimental observation of residual correlation presented above confirms this view. In short, one may define the peak of Fig. 2, as an n-n correlation peak. By using denominator A, we obtained a correlation function corresponding to $r_0 = 5$ fm close to that (5.3 fm) obtained in Ref. [21]. Here r_0 represents the variance of the Gaussian source assumed in the model of Ref. [20]. The

n-n separation r_{nn} is a Gaussian distribution of variance $\sqrt{2}r_0$ and $r_{nn}^{\mathrm{rms}}=\sqrt{6}r_0$. It follows that $r_0\sim 5$ leads to $r_{nn}^{\mathrm{rms}}\sim 13$ fm. This is an inflated value due to residual correlation that produces an increase of denominator *A*. By using denominator *B*, we obtained a correlation function corresponding to $r_0=4.2$ fm, leading to $r_{nn}^{\mathrm{rms}}=10.2$ fm, which is not far from $r_{nn}^{\mathrm{rms}}=8.3$ fm predicted by $\mathrm{COSMA_I}$ model [5]. One has to point out that the initial denominator obtained in Ref. [17] corresponds to the same $r_0=4.2$ fm value as in the case of our denominator *B* (see the inset in Fig. 5 for ^{11}Li, Ref. [17]). We have tried to understand why in Ref. [17] the same initial denominator as in Ref. [21] or in our case (denominator *A*) was not obtained. We have found that in Ref. [21] and in our case the geometrical conditions of measurements were such that the angles subtended by one detector were nearly the same $\sim 1.6°$. In the case of Ref. [17] this angle was about 1.7 times larger, and therefore a smoothing of residual correlation could take place, so that the correlation function corresponded not to $r_0=5$ fm, but to $r_0=4.2$ fm. A similar smoothing took place in our case for denominator *B* by taking a distribution of detectors not a random one, but a particular distribution corresponding to the measured sample of *n-n* coincidences. In Ref. [17] an elegant iteration procedure was worked out for getting the intrinsic correlation function from the measured one. In this iterative procedure are implied all the measured $C(q_i)$ values with their experimental errors. Finally the reconstructed correlation function appears with substantially increased errors in comparison with the initial one. We have applied this method starting with the correlation function defined by $r_0=4.2$ fm. We have found a stable solution corresponding to $r_0=3.3\pm 0.8$ fm [22], in good agreement with the value obtained in Ref. [17] (2.7 ± 0.6 fm). In Fig. 5(b) is represented by down-triangles the shape of the denominator obtained by this calculation.

We consider that at present a challenging task is to try to distinguish between the r_0 predicted by $\mathrm{COSMA_I}$ and by $\mathrm{COSMA_{II}}$ models [5]. An answer to this question will be an experiment aiming to determine the intrinsic correlation function by using ^{11}Li and ^{11}Be halo nuclei. The ^{11}Be nucleus will be an ideal uncorrelated background source, since it contains only one halo neutron. This experiment should be done by using a ^{12}C instead a Si target. A sharp cutoff estimation [23] has indicated that the *n-n* correlation peak will be about two times higher in the case of ^{12}C than in the case of the Si target.

The experimentally observed signatures of residual correlation could be of use in the identification of new halo nuclei [24].

M.P. and A.I. acknowledge IFA and IFIN-HH authorities for CERES projects 51 and 80 supporting this research. M.P is grateful to Professor P. Desesquelles for MENATE program, and to Dr. F. M. Marques for sending him part of a manuscript prior to publication. M.P., H.P., A.I., I.C., acknowledge Professor S. Kobayashi, President of RIKEN, for support during preparation and performing of this experiment.

[1] I. Tanihata *et al.*, Phys. Lett. **160B**, 380 (1985).
[2] M. Petrascu *et al.*, Balkan Phys. Lett. **3**(4), 214 (1995).
[3] M. Petrascu *et al.*, Phys. Lett. B **405**, 224 (1997).
[4] M. Petrascu *et al.*, Rom. J. Phys. **44**, 83 (1999).
[5] M. V. Zhukov *et al.*, Phys. Rep. **231**, 151 (1993).
[6] S. Koonin, Phys. Lett. **70B**, 43 (1977).
[7] H. Petrascu *et al.*, Rom. J. Phys. **44**, 105 (1999).
[8] M. Petrascu *et al.*, Rom. J. Phys. **44**, 115 (1999).
[9] M. Petrascu, *Proceedings of International Symposium on Exotic Nuclei, Baikal-Lake, Russia, 2001* (World Scientific, Singapore, 2002), p. 256.
[10] M. Petrascu *et al.*, preprint RIKEN-AF-NP-395, 2001.
[11] N. Colonna *et al.*, Phys. Rev. Lett. **75**, 4190 (1995).
[12] R. Ghetti *et al.*, Nucl. Instrum. Methods Phys. Res. A **421**, 542 (1999).
[13] P. Desesquelles, the program MENATE (unpublished).
[14] M. Petrascu *et al.*, Nucl. Instrum Methods (unpublished).
[15] G. I. Kopylov, Phys. Lett. **50B**, 472 (1974).
[16] R. Ghetti *et al.*, Nucl. Phys. **A660**, 20 (1999).
[17] F. M. Marques *et al.*, Phys. Lett. B **476**, 219 (2000).
[18] M. Petrascu, in *Proceedings of the International Seminar on Heavy Ion Physics (HIPH'02) Dubna, Russia, 2002*, edited by Yu. Ts. Oganessian and R. Kalpakchieva (Yad. Fiz., in press).
[19] M. Petrascu *et al.*, in *Proceedings of the International Seminar on Heavy Ion Physics (HIPH'02) Dubna, Russia, 2002* (Ref. [18]) abstracts, p. 79.
[20] R. Lednicky and L. Lyuboshits, Sov. J. Nucl. Phys. **35**, 770 (1982).
[21] K. Ieki *et al.*, Phys. Rev. Lett. **70**, 730 (1993).
[22] M. Petrascu *et al.* (unpublished).
[23] M. Petrascu *et al.* (unpublished).
[24] M. Petrascu *et al.* (unpublished).